Available online at www.sciencedirect.com
SCIENCE DIRECT
Surface Science 600 (2006) 1837–1848
SURFACE SCIENCE
www.elsevier.com/locate/susc

The chemistry of ethylene on MoAl alloy thin films formed on dehydroxylated alumina: Hydrogenation, dehydrogenation and H–D exchange reactions

Feng Gao, Yilin Wang, Luke Burkholder, W.T. Tysoe *

Department of Chemistry and Biochemistry, and Laboratory for Surface Studies, University of Wisconsin-Milwaukee, 3210 N Cramer Street, Milwaukee, WI 53211, USA

Received 10 November 2005; accepted for publication 9 February 2006
Available online 3 March 2006

Abstract

The chemistry of ethylene adsorbed on a thin MoAl layer grown in ultrahigh vacuum on a thin alumina film is studied using a combination of temperature-programmed desorption and X-ray, Auger and reflection absorption infrared spectroscopies. Both di-σ-bonded and a small proportion of π-bonded ethylene are found, where the di-σ-bonded ethylene has a σ/π parameter of ~0.8 and a heat of adsorption of ~70 kJ/mol. The ethylene self-hydrogenates to yield ethane and a small amount of methane is detected. The surface hydrogenation activation energy of di-σ-bonded ethylene is ~65 kJ/mol, while the π-bonded species hydrogenates more easily. Adsorbed ethyl species grafted onto the surface by decomposing ethyl iodide predominantly undergo β-hydride elimination to yield ethylene. Ethyl species hydrogenate to ethane at a lower temperature than does di-σ-bonded ethylene implying that addition of hydrogen to adsorbed ethylene is slower than the rate of ethyl hydrogenation.

Keywords: X-ray photoelectron spectroscopy; Temperature-programmed desorption; Auger spectroscopy; Reflection–absorption infrared spectroscopy; Chemisorption; Molybdenum hexacarbonyl; Alumina thin films; Ethylene; Iodoethane

1. Introduction

$Mo(CO)_6$ has been extensively used to deposit molybdenum on oxides to generate catalysts and/or catalyst precursors [1–12]. Such a procedure has been applied in ultrahigh vacuum to generate model catalysts supported on planar alumina thin films, where surface-sensitive spectroscopic probes can be exploited to investigate the surfaces and catalytic reactions [13–16]. Our recent studies have shown that reacting $Mo(CO)_6$ with aluminum [17] and dehydroxylated and hydroxylated alumina [18,19] thin films at 700 K deposits molybdenum carbide incorporating a small amount of oxygen. It has also been shown that reaction of low exposures of $Mo(CO)_6$ with alumina thin films results in the formation of small molybdenum carbide particles, while higher exposures (~5000 L of $Mo(CO)_6$) leads to a thin carbide film that completely covers the surface [18]. Annealing these films to temperatures up to 1500 K causes CO desorption through alumina reduction by the carbidic carbon, and results in MoAl alloy film formation [17–19].

Organic iodides have been extensively used to examine the surface chemistry of hydrocarbons since these tend to decompose by scission of the C–I bonds at relatively low temperatures to deposit hydrocarbon fragments, along with chemisorbed iodine [20,21]. We have recently investigated the chemistry of iodomethane [22] and diiodomethane [23] on MoAl alloy thin films and found that besides hydrogen and methane formation, some ethylene, ethane, propylene (from both iodomethane and diiodomethane) and butene (just from diiodomethane) are formed. These products are suggested to form via methylene

* Corresponding author. Tel.: +1 414 229 5222; fax: +1 414 229 5036.
E-mail address: wtt@uwm.edu (W.T. Tysoe).

0039-6028/$ - see front matter © 2006 Elsevier B.V. All rights reserved.
doi:10.1016/j.susc.2006.02.015

insertion into alkyl-metal bonds followed by β-hydride or reductive elimination reactions [24,25]. Methylene is formed by partial decomposition of adsorbed methyl groups through C–H bond cleavage following iodomethane adsorption [22], or alternatively by C–I bond dissociation following diiodomethane adsorption. In this latter case, surface methyls are formed by hydrogenation of methylene species [23].

Thus the molybdenum–aluminum alloy surfaces are extremely effective for methylene insertion into surface–carbon single bonds to form higher alkyl groups. This implies that these surfaces may also be similarly active for methylene insertion into the carbon–surface bond of di-σ-bonded olefins to yield metallacycles. Metallacycles have been proposed to be the central intermediates in olefin metathesis catalysis, where the reverse of the insertion reaction forms metathesis products. Such a mechanism was first proposed by Herisson and Chauvin [26] and recently confirmed for the heterogeneous phase in ultrahigh vacuum on model molybdenum carbide catalysts [27,28]. As a precursor to investigating this chemistry, the reactivity of ethylene alone on the MoAl alloy is explored to investigate hydrogenation and H–D exchange activities. Since, according to the Horiuti–Polanyi mechanism [29], ethane must necessarily form via an ethyl intermediate, the chemistry of ethyl species is also explored using iodoethane as a precursor.

The formation and characterization of MoAl alloy films has recently been extensively described [18]. Briefly, it is formed by adsorbing 5000 L of $Mo(CO)_6$ onto a dehydroxylated alumina film grown on a Mo(100) substrate held at 700 K to generate a molybdenum carbide film. This is then annealed to 1500 K to generate a surface MoAl alloy. During the annealing process, the deposited carbidic carbon reacts completely with the alumina substrate to form CO, reducing it to metallic aluminum. Alloy formation is confirmed by X-ray photoelectron and Auger spectroscopies where it is found that the binding energy of the deposited molybdenum, following annealing, is lower than that of pure metallic molybdenum [17,18]. The thickness of the alloy film, based on Auger electron probe depth analysis, is estimated to be 3–4 atomic layers [22].

2. Experimental

Temperature-programmed desorption (TPD) data were collected in an ultrahigh vacuum chamber operating at a base pressure of 8×10^{-11} Torr that has been described in detail elsewhere [13,17,18] where desorbing species were detected using a Dycor quadrupole mass spectrometer placed in line of sight of the sample. Temperature-programmed desorption spectra were collected at a heating rate of 10 or 15 K/s. This chamber was also equipped with a double-pass cylindrical mirror analyzer for obtaining Auger spectra. These are typically collected using an electron beam energy of 3 keV and the first derivative spectra are obtained by numerical differentiation.

X-ray photoelectron spectra (XPS) were collected in another chamber operating at a base pressure of 2×10^{-10} Torr, which was equipped with Specs X-ray source and double-pass cylindrical mirror analyzer. Spectra were typically collected with an Mg Kα X-ray power of 250 W and a pass energy of 50 eV. The alumina substrate was sufficiently thin that no charging effects were found and the binding energies were calibrated using the Mo $3d_{5/2}$ feature (at 227.4 eV binding energy) as a standard [17,18]. Temperature-dependent XP and Auger spectra were collected by heating the sample to the indicated temperature for 5 s, allowing the sample to cool to 150 K, following which the spectrum was recorded.

Infrared data were collected using a Bruker Equinox infrared spectrometer equipped with a liquid-nitrogen-cooled, mercury cadmium telluride detector operated at 4 cm^{-1} resolution and data were typically collected for 1000 scans. The complete light path was enclosed and purged with dry, CO_2-free air [15,16].

The Mo(100) substrate (1 cm diameter, 0.2 mm thick) was cleaned using a standard procedure, which consisted of argon ion bombardment (2 kV, 1 μA/cm^2) and any residual contaminants were removed by briefly heating to 2000 K in vacuo. The resulting Auger spectrum showed no contaminants. Aluminum was deposited onto Mo(100) from a small heated alumina tube, which was enclosed in a stainless-steel shroud to minimize contamination of other parts of the system [30]. Alumina thin films were formed by cycles of aluminum deposition-water vapor oxidation-annealing, until the Mo(100) XPS or AES features were completely obscured [18].

Molybdenum hexacarbonyl (Aldrich, 99%), ethylene (Matheson, 99.5%), d_4-ethylene (Cambridge Isotope, 99% D) and iodoethane (Aldrich, 99%) were transferred to glass vials, connected to the gas-handling line of the chamber and purified by repeated freeze-pump-thaw cycles, followed by distillation, and their purities were monitored using mass spectroscopy. These were dosed onto the surface via a capillary doser to minimize background contamination. The exposures in Langmuirs ($1\ L = 1 \times 10^{-6}$ Torr s) are corrected using an enhancement factor determined using temperature-programmed desorption (see [13] for a more detailed description of this procedure). H_2 and D_2 (Matheson, $\geqslant$99.5%) were used without further purification.

3. Results

Fig. 1 displays the (a) 26, (b) 27 and (c) 28 amu desorption spectra for ethylene adsorbed on the molybdenum aluminum alloy at 150 K as a function of ethylene exposure, collected using a heating rate of 10 K/s. Data were also collected at 24 and 25 amu but not displayed. The relative intensities at these masses are identical to the fragmentation pattern of pure ethylene measured with the same mass spectrometer, confirming these profiles are due to ethylene desorption except for some additional intensity at ~170 K

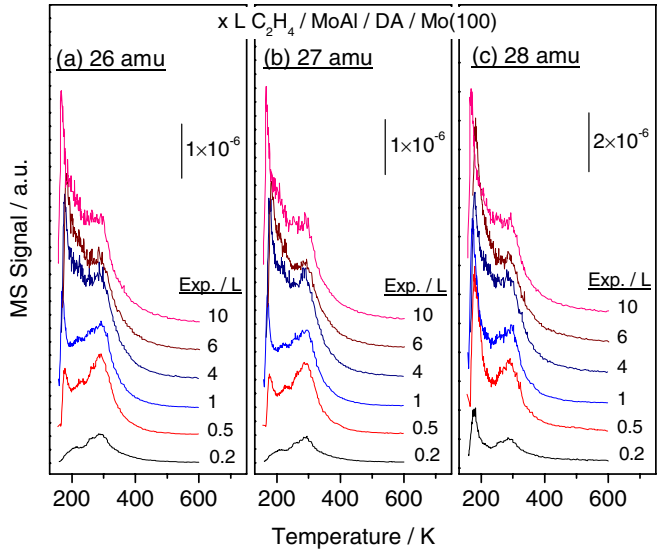

Fig. 1. (a) 26, (b) 27 and (c) 28 amu temperature-programmed desorption spectra of ethylene adsorbed on a MoAl film at 150 K collected using a heating rate of 10 K/s, as a function of ethylene exposure. Ethylene exposures are marked adjacent to the corresponding spectrum.

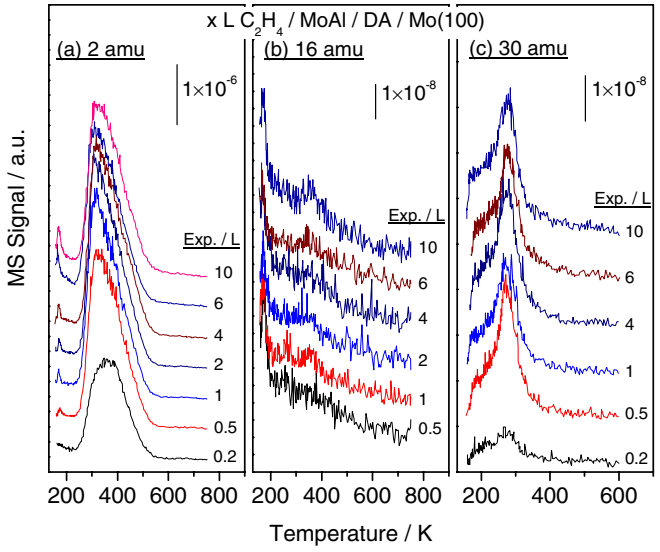

Fig. 2. (a) 2 (H_2), (b) 16 (CH_4) and (c) 30 (C_2H_6) amu temperature-programmed desorption spectra of ethylene adsorbed on a MoAl film at 150 K collected using a heating rate of 10 K/s, as a function of ethylene exposure. Ethylene exposures are marked adjacent to the corresponding spectrum.

at 28 amu due to some CO desorption originating from background CO. Two major C_2H_4 desorption states are found. A low-temperature state centered at ~210 K is observed at an ethylene exposure of 0.2 L, which shifts to ~175 K at exposures of 0.5 L and above. A high-temperature state is found at ~285 K independent of ethylene exposure. An additional weaker desorption peak is found centered at ~220 K at ethylene exposures of 0.5 and 1 L, which is obscured by the two stronger desorption peaks at higher ethylene exposures. This state is not detected at 28 amu since it is obscured by the low-temperature CO and ethylene peaks. We also tentatively assign this state to ethylene.

The desorption of other products is displayed in Fig. 2 where Fig. 2(a) shows the 2 amu (H_2) profiles as a function of ethylene exposure. H_2 desorption occurs between 300 and 550 K with a peak maximum at 330 K. The H_2 yield reaches a maximum at an ethylene exposure of ~1 L and decreases slightly thereafter. It should be mentioned that, although the majority of desorbed H_2 comes from ethylene decomposition, a small portion originates from background H_2 adsorption. By carrying out blank experiments, it was found that background H_2 desorbs at ~400 K where, at an ethylene exposure of 0.2 L, background H_2 comprises ~40% of the total H_2 desorbed. The percentage decreases to less than ~20% at C_2H_4 exposures of 0.5 L and higher. Shown in Fig. 2(b) is the corresponding 16 amu (CH_4) desorption profiles. Weak yet detectable methane desorption occurs at ~350 K for C_2H_4 exposures of 0.5 L and above. Again, the ~170 K state at 16 amu is due to CO desorption shown in Fig. 1(c). Finally, Fig. 2(c) plots the 30 amu (ethane) desorption profiles. The majority of the ethane desorbs at ~270 K, ~15 K lower than the desorption maximum of strongly bound ethylene (Fig. 1). The ethane yield reaches a maximum at an ethylene exposure of 0.5 L, and decreases slightly at higher exposures. It is also found that some ethane desorbs as low as ~180 K. Presumably ethane is formed by self-hydrogenation of ethylene, where a portion of chemisorbed ethylene dissociates to provide surface hydrogen. Since background hydrogen also adsorbs on the surface, this chemistry is also facilitated to some extent by background hydrogen adsorption. No other gaseous hydrocarbons or oxygenates are found to desorb.

In order to further investigate ethylene hydrogenation, the surface chemistry of ethylene is investigated on both H_2- and D_2-presaturated surface. The alloy surface is exposed to ~20 L of H_2 at 200 K to avoid CO adsorption from the background [22,23] and the sample is allowed to cool to ~150 K before ethylene adsorption. Fig. 3(a) plots the resulting H_2 (2 amu) desorption profiles as a function of ethylene exposure. It is observed that the amount of H_2 desorbed from the surface does not vary substantially with ethylene exposures. Fig. 3(b) displays ethylene desorption (at 27 amu) as a function of exposure where similar desorption profiles are found as for ethylene desorption from the bare surface (Fig. 1). In this case, two desorption states are found at ~170 and ~280 K, respectively. It is evident, however, that the ethylene yield from a hydrogen-covered surface is larger than that from the clean surface at the same ethylene exposure, suggesting that co-adsorbed hydrogen inhibits the extent of ethylene decomposition. As shown in Fig. 3(c), ethane desorbs at ~260 K, ~10 K lower than from the bare surface, and the yield is ~5 times greater. Finally, no methane, other gaseous hydrocarbons nor oxygenates were found to desorb from the hydrogen-covered surface.

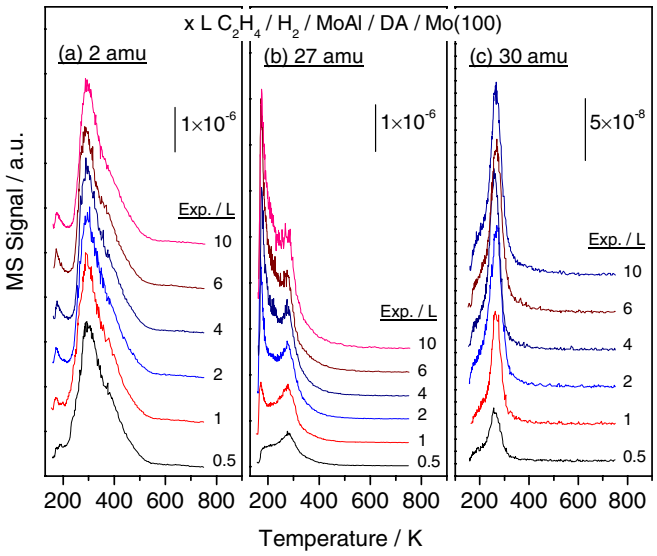

Fig. 3. (a) 2 (H_2), (b) 27 (C_2H_4) and (c) 30 (C_2H_6) amu temperature-programmed desorption spectra of ethylene adsorbed on a MoAl film saturated with 20 L of H_2 at 150 K collected using a heating rate of 10 K/s, as a function of ethylene exposure. Ethylene exposures are marked adjacent to the corresponding spectrum.

The resulting desorption profiles at a number of masses for ethylene hydrogenation by deuterium are displayed in Fig. 4, following a 10 L ethylene exposure to the alloy surface predosed with 20 L of D_2. Desorption at 32 amu, centered at ~286 K, is observed. Desorption at the same temperature is also found at 29, 30 and 31 amu. A

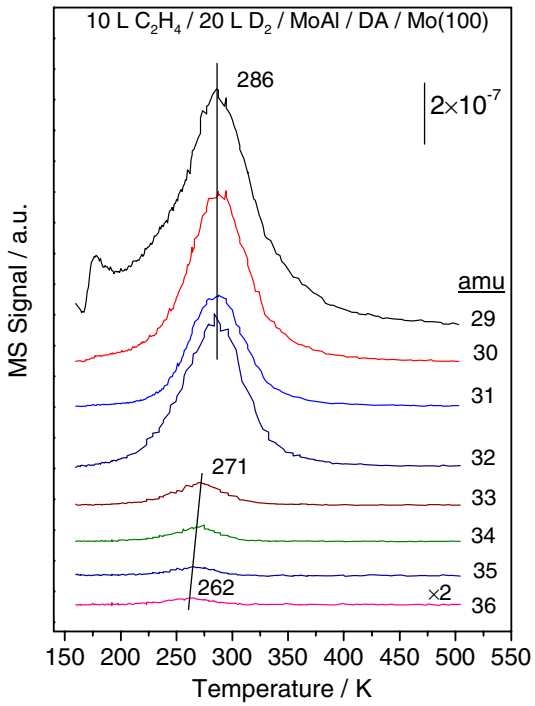

Fig. 4. 29–36 amu temperature-programmed desorption spectra following a 10 L C_2H_4 exposure to a MoAl surface saturated with 20 L of D_2 at 150 K.

fragment at 32 amu could be due either to hydrogenation ($C_2H_4D_2$) or to H–D exchange products (C_2D_4). As will be shown below, the intense features at 32 amu and lower are due to ethylene that has undergone rapid H–D exchange. This is further confirmed by carrying out experiments with C_2D_4 on a H_2-covered surface (data not shown). Weaker but easily detectable features are found at 33, 34, 35 and 36 amu due to ethane from hydrogenation of ethylene that has exchanged with surface deuterium. Desorption at 35 and 36 amu can be definitively assigned to C_2HD_5 and C_2D_6, respectively. The slightly higher desorption temperatures and larger intensities at 33 and 34 amu suggest that C_2HD_5 and C_2D_6 do not contribute much to these two masses and these can be assigned to $C_2H_3D_3$ and $C_2H_2D_4$, respectively. It is worth pointing out that the desorption temperatures of ethylene isotopomers are slightly higher than those of the ethane isotopomers.

Since ethylene hydrogenation invariably proceeds via a surface ethyl intermediate, the surface chemistry of ethyl species is investigated by adsorbing iodoethane on the surface [20,21]. Fig. 5(a) displays the 29 amu ($C_2H_5^+$) desorption profiles as a function of C_2H_5I exposure, which represents mainly molecular desorption. As will be shown below, ethane, which has a fragment at 29 amu, also forms. However, the desorption line shapes at 63 amu (I^{2+}) (not shown) are almost identical to those at 29 amu, indicating that the ethane contribution to the 29 amu feature is small. At an iodoethane exposure of 1 L, molecular desorption occurs at ~242 K. This temperature decreases with increasing exposure, so that at an exposure of 3.5 L and above, it shifts to ~225 K. It is also found that, at an iodoethane exposure of 10 L, extensive desorption occurs at ~186 K and increases indefinitely with increasing iodoethane exposure so that this state is assigned to multilayer desorption. Thirty atomic mass unit (C_2H_6) desorption profiles are displayed in Fig. 5(b) where it is found that the desorption temperature also decreases with increasing iodoethane exposure. A desorption maximum is found at ~253 K at low exposure (1 L), which decreases to ~210 K at the highest exposure (10 L). The peak at 186 K at the highest exposure is likely to be a fragment of the parent molecule. Desorption at 27 amu is also investigated to monitor ethylene formation and the results are plotted in Fig. 5(c). Although iodoethane itself has a fragment at 27 amu, the high-temperature tails extending up to 450 K strongly suggests ethylene formation. An inset in Fig. 5(c) compares the desorption profiles of 27, 29 and 30 amu at an iodoethane exposure of 1 L. This clearly demonstrates ethylene formation via ethyl dehydrogenation is substantially more facile than hydrogenation.

Ethane formation from ethyl species is also investigated on H_2 (D_2) saturated surfaces and the results are plotted in Fig. 6. Fig. 6(a) displays the ethane (30 amu) desorption spectra from a H_2-covered alloy surface where ethane desorbs at ~230 K following an iodoethane exposure of 1 L, and decreases to ~210 K at the highest exposure. At every

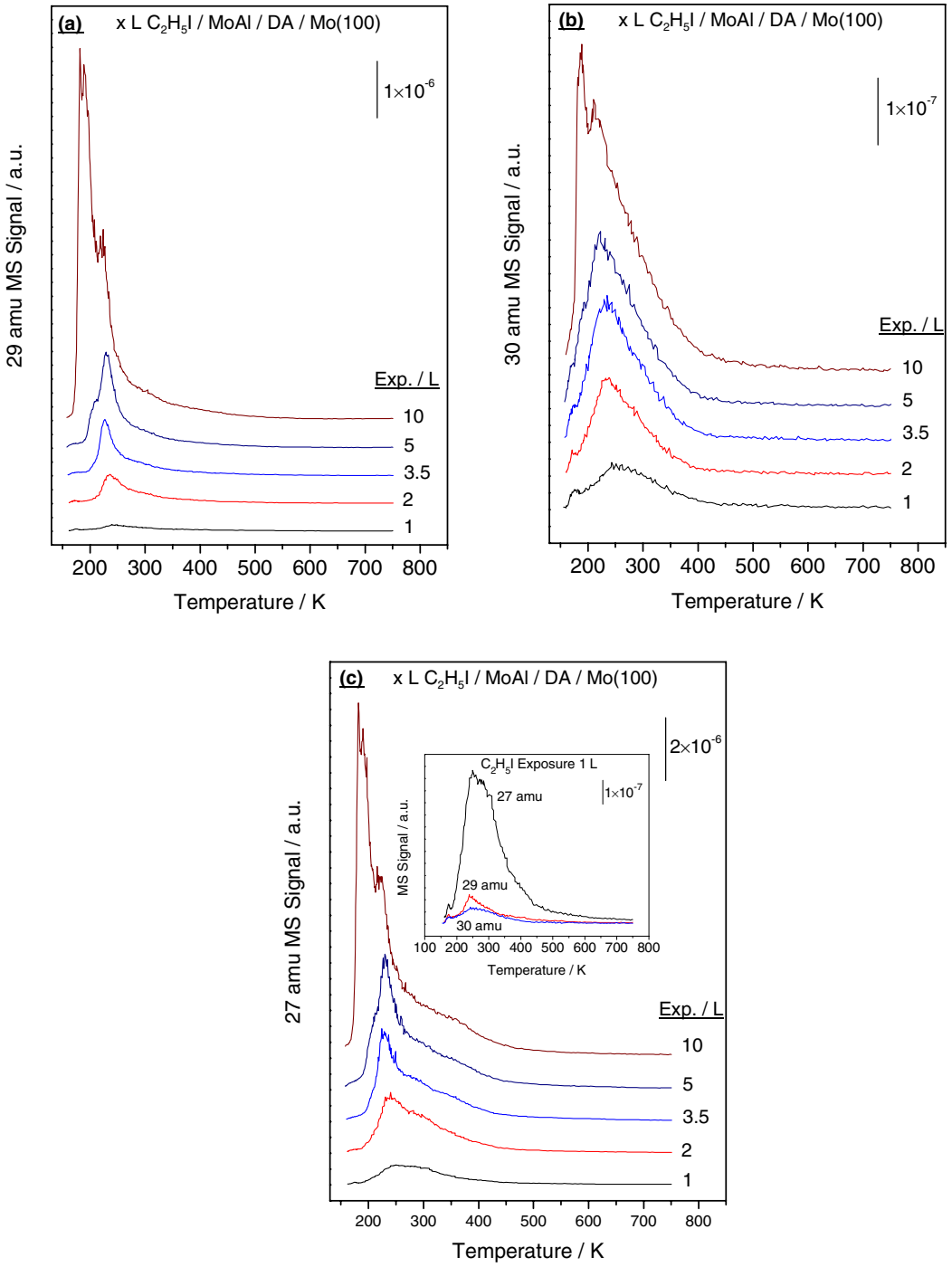

Fig. 5. (a) 29 (C_2H_5), (b) 30 (C_2H_6) and (c) 27 amu temperature-programmed desorption spectra of iodoethane adsorbed on a MoAl film at 150 K collected using a heating rate of 10 K/s, as a function of iodoethane exposure. Iodoethane exposures are marked adjacent to the corresponding spectrum. The inset to (c) compares the 27, 29 and 30 amu profiles at an iodoethane exposure of 1 L.

iodoethane exposure, the ethane yield almost tripled on the hydrogen-covered surface compared with that on the bare surface (Fig. 5(b)) (note the different sensitivity scales in the two figures). Fig. 6(b) presents the results on a deuterium-covered surface monitoring 30, 31, 32 and 33 amu. It is found that, while 32- and 33-amu profiles display only one state centered at ~310 and ~290 K, respectively, 30- and 31-amu profiles show two desorption states. The high-temperature state is centered at ~310 K irrespective of iodoethane exposure, while the low-temperature state decreases in desorption temperature with increasing iodoethane exposure, so that at an iodoethane exposure of 3.5 L, it is at ~230 K while at an iodoethane exposure of 10 L, it decreases to ~210 K. At the lowest iodoethane exposure (1 L), this state appears as a shoulder on the high-temperature desorption state so that the desorption peak

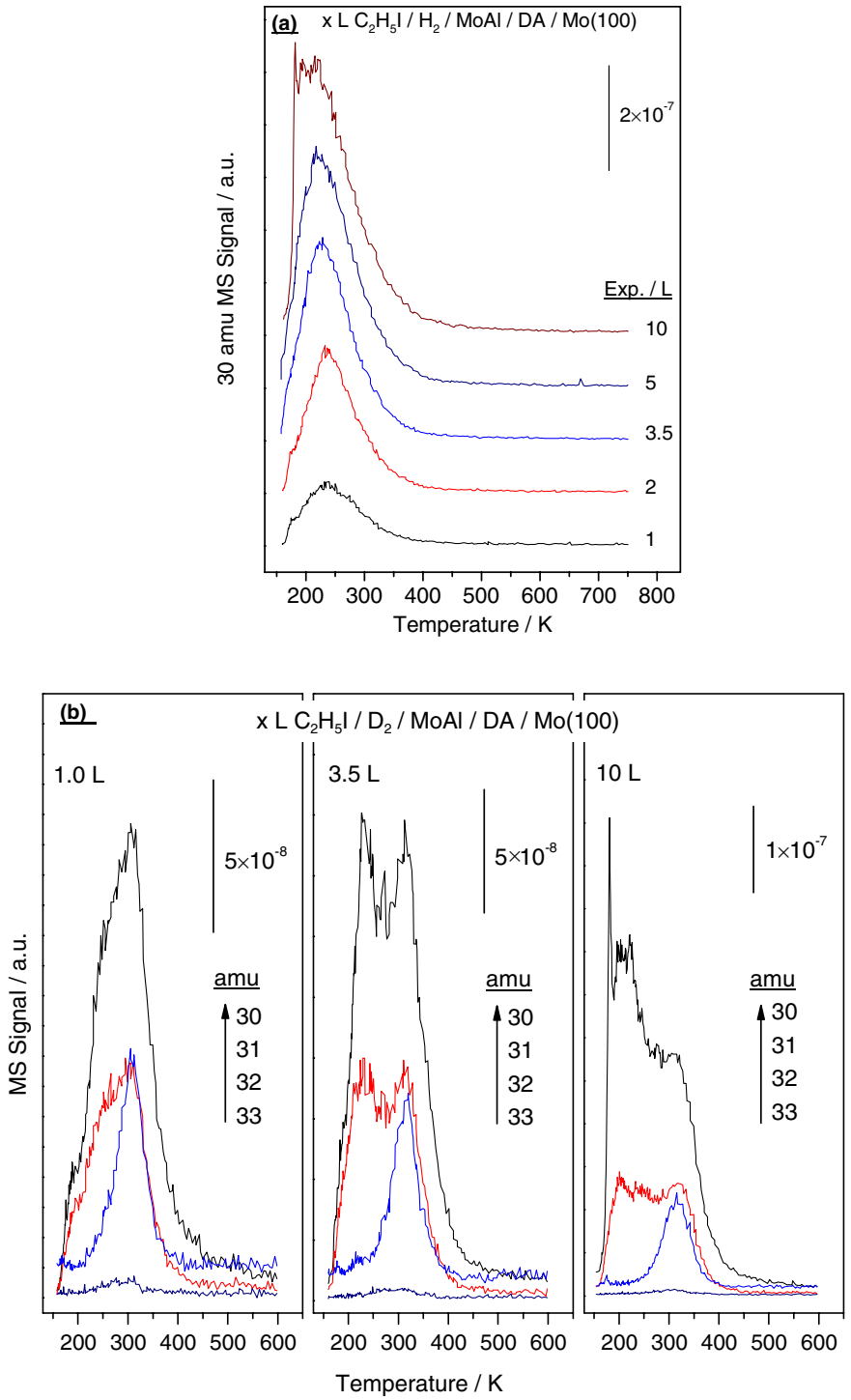

Fig. 6. (a) 30 (C_2H_6) amu temperature-programmed desorption spectra following C_2H_5I adsorption on a MoAl surface presaturated with 20 L of H_2 at 150 K. C_2H_5I exposures are marked adjacent to the corresponding spectrum. (b) 30–33 amu temperature-programmed desorption spectra following C_2H_5I adsorption on a MoAl surface presaturated with 20 L of D_2 at 150 K. C_2H_5I exposures are 1, 3.5 and 10 L.

maximum temperature cannot be measured. The nature of the desorbed products will be discussed in greater detail below.

The surface chemistry of ethylene and iodoethane is further investigated using Auger, X-ray photoelectron (XPS) and reflection–absorption infrared (RAIRS) spectroscopies. Fig. 7(a) displays the RAIRS of 10 L of ethylene adsorbed on the alloy surface at 80 K and subsequently annealed to higher temperatures. All spectra are collected at 80 K and the annealing temperatures are indicated adjacent to the corresponding spectrum. It should be mentioned that an intense and wide alumina LO mode [31] centered at ~930 cm^{-1} is detected preventing meaningful spectra from being collected at frequencies below 1000 cm^{-1}. Following

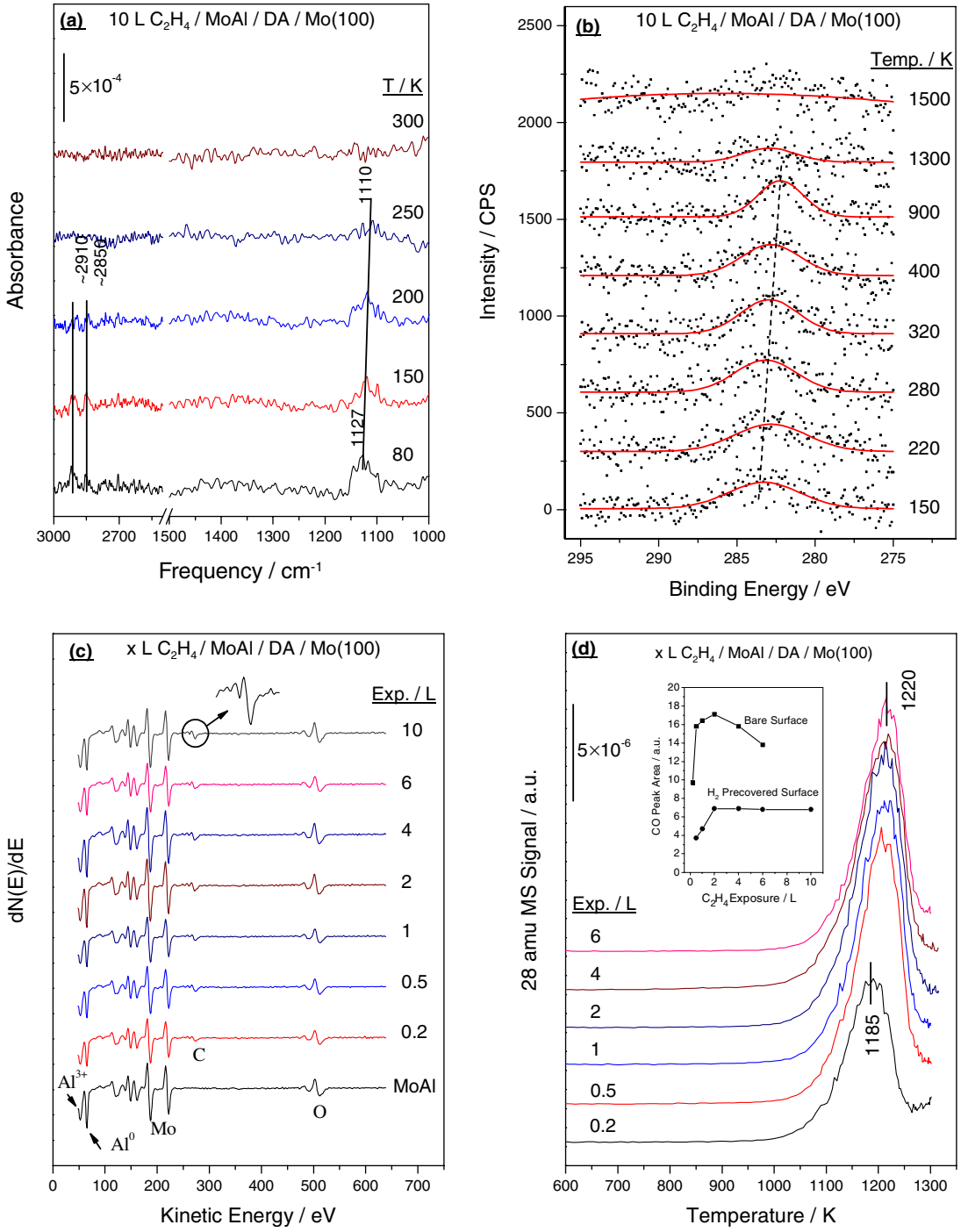

Fig. 7. (a) RAIRS of 10 L of ethylene adsorbed on an alloy surface at 80 K and annealed to various temperatures. The annealing temperatures are displayed adjacent to the corresponding spectrum. (b) Narrow scan X-ray photoelectron spectra of the C 1s region following a 10 L ethylene exposure to an alloy surface at 150 K and annealed to various temperatures. The annealing temperatures are displayed adjacent to the corresponding spectrum. (c) A series of Auger spectra plotted as a function of ethylene exposure, where exposures are marked adjacent to the corresponding spectrum, collected following ethylene adsorption on a MoAl alloy film at 150 K and annealing to 750 K. The spectra were collected after allowing the sample to cool to 150 K. Shown also is an enlarged carbon KLL Auger spectrum. (d) 28 (CO) amu temperature-programmed desorption spectra of ethylene adsorbed on a MoAl film at 150 K and then annealed to 750 K, collected using a heating rate of 15 K/s, as a function of C_2H_4 exposure. Ethylene exposures are marked adjacent to the corresponding spectrum. Shown as an inset is the integrated CO desorption yields as a function of ethylene exposure, on both bare and H_2-presaturated surfaces.

ethylene adsorption at 80 K, features are observed at ~2910, ~2850 and ~1127 cm^{-1} (Fig. 7(a)). The two high-frequency modes persist on heating to 200 K and, by 250 K, they disappear. The low-frequency mode is still detected at 250 K while there is a slight red shift during annealing, but disappears on heating to 300 K.

The XPS data are displayed in Fig. 7(b) where, due to the low cross-section of surface carbon, the C 1s signal is very weak. A C 1s binding energy of 283.6 eV is observed at 150 K and shifts to lower energies at higher temperatures. At temperatures above 400 K, the observed binding energy of 282.7 eV indicates the presence of carbidic carbon. This clearly demonstrates that a portion of the adsorbed ethylene undergoes complete dissociation to leave carbon atoms on the surface at high temperatures. This chemistry is also monitored using Auger spectroscopy following TPD experiments after the sample had been heated to above 750 K, and the results are shown in Fig. 7(c). Upon ethylene adsorption and annealing, a weak signal is detected at ~270 eV, indicating carbon deposition. An enlarged carbon KLL region reveals a line shape characteristic of carbidic carbon [18]. Identical experiments performed on a hydrogen-presaturated surface also reveal carbon deposition (data not shown). Due to the low carbon signal intensities, no effort was made to plot carbon uptake from the Auger data. The residual carbon on the surface is monitored with greater sensitivity using TPD where CO is evolved at ~1200 K due to a reaction between the carbidic carbon and oxygen from the alumina substrate [17–19] and the results are plotted in Fig. 7(d). It is found that, at the lowest ethylene exposure, CO desorbs at 1185 K, where the temperature increases slightly to 1220 K at larger ethylene exposures. Shown as an inset is the CO desorption peak area as a function of ethylene exposure, for both clean and hydrogen-presaturated surfaces. This clearly demonstrates that in both cases, carbon deposition reaches a maximum at ethylene exposures of ~2 L. In addition, it is found that ethylene dissociation is inhibited by surface hydrogen, consistent with TPD results (Figs. 1 and 3).

Fig. 8(a) displays the corresponding RAIRS data for C_2H_5I adsorbed on the alloy surface at 80 K and subsequently annealed to higher temperatures. At an exposure of 1 L at 80 K, relatively intense features are detected at 2974, 2924 and 2865 cm^{-1} in the C–H stretching region accompanied by less intense peaks at 2958, 2910 and 2854 cm^{-1}. At lower frequencies, features are detected at 1441, 1432 (shoulder), 1377 and 1202 cm^{-1}. At an exposure of 10 L (above monolayer saturation), intense peaks are detected at 3010, 2968, 2913 and 2853 cm^{-1} in the C–H stretching region with shoulders at 2954, 2924 and 2864 cm^{-1}. At lower frequencies, strong features are detected at 1438, 1373 and 1202 cm^{-1} accompanied by smaller peaks adjacent to the 1438 cm^{-1} feature at 1453 and 1425 cm^{-1}. As the sample is annealed to 150 K, besides the features detected at 80 K, a new weak feature appears at 2883 cm^{-1}, and the 2954 cm^{-1} shoulder at 80 K develops into a well-resolved peak. At the same time, the 3010 and 2968 cm^{-1} features shift to 3017 and 1976 cm^{-1}, respectively. In the low frequency region, the shoulders at 1453 and 1425 cm^{-1} develop into clearly resolved peaks, and a new feature appears at 1476 cm^{-1}. The assignments of these absorbances at 80 K are given in Table 1. All these features disappear on annealing to 200 K leaving a weak and broad peak centered at ~1112 cm^{-1}. This feature disappears when the sample is annealed to 250 K and above (data not plotted), as found for adsorbed ethylene in Fig. 7(a).

Fig. 8(b) shows I $3d_{5/2}$ XPS data for 10 L of iodoethane adsorbed at 150 K and subsequently annealed to higher temperatures. Again the annealing temperatures are indicated adjacent to the corresponding spectrum. The I $3d_{5/2}$ binding energy is 620.1 eV at 150 K. As the sample is annealed to 220 K, the signal intensity decreases drastically accompanied with a binding energy shift to 619.4 eV. From 220 to 900 K, no apparent signal intensity decrease is observed, but a slight binding energy increase is found. A drastic signal intensity decrease is found again at 1100 K and by 1300 K, all iodine has desorbed. Fig. 8(c) displays the corresponding C 1s XPS data showing a feature centered at 284.4 eV at 150 K. Similar to the behavior of iodine, the signal intensity decreases at 220 K together with a binding energy shift to 283.6 eV. A further binding energy decrease is found at 300 K and above and finally the carbon signal disappears at above 1300 K.

4. Discussion

The ethylene hydrogenation reaction pathway has been studied extensively on well-defined single crystal surfaces of various transition metals [20,21]. It is generally agreed that ethylene hydrogenation proceeds via a surface ethyl intermediate according to the Horiuti–Polanyi mechanism [29]. Fig. 1 reveals that ethylene desorbs in two states, the first being a sharp state with a peak temperature of ~170–210 K depending on ethylene exposure, and a higher-temperature state centered at ~285 K. The onset of the sharp, low-temperature state occurs immediately when the temperature ramp is initiated suggesting that the real peak of this desorption state is below the adsorption temperature. This feature disappears when the sample was previously heated very slowly to above 200 K indicating that this feature arises from ethylene desorption from the alloy surface and not the sample support. A Redhead analysis [32] of the higher-temperature (~285 K) state yields a desorption activation energy of ~70 kJ/mol. The infrared spectra of ethylene adsorbed on the MoAl alloy at 80 K (Fig. 7(a)) reveals a broad feature centered at ~1127 cm^{-1} and sharper features in the C–H stretching region at ~2910 and 2850 cm^{-1}. The breadth of the 1127-cm^{-1} mode indicates that there is some surface heterogeneity in adsorption sites. This is assigned to the CH_2 wagging mode of di-σ-bonded ethylene, where this frequency indicates that the adsorbed ethylene has a $\sigma - \pi$ parameter of ~0.8, similar to that on a ruthenium surface [33]. The 2901 cm^{-1} feature is assigned to a symmetric CH_2 stretch mode. The origin of the ~2850 cm^{-1} mode is not clear, but may be an overtone. The CH_2 wagging mode decreases slightly in frequency to ~1110 cm^{-1} and decreases substantially in intensity on heating to ~250 K, indicating that this mode is associated with the ~285 K desorption state (Fig. 1) and its complete disappearance at 300 K

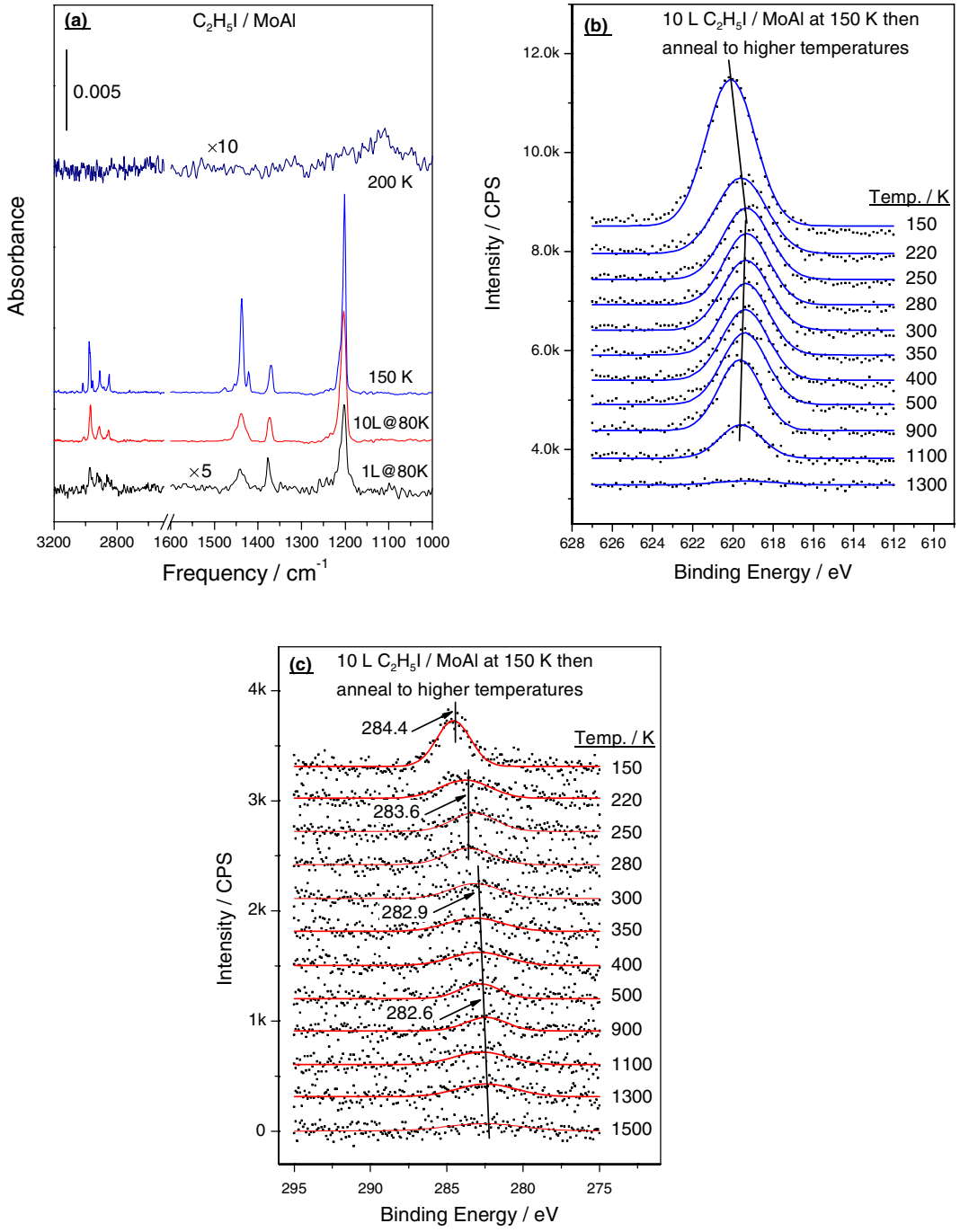

Fig. 8. (a) RAIRS of iodoethane adsorbed on an alloy surface at 80 K and annealed to various temperatures. The exposures and annealing temperatures are displayed adjacent to the corresponding spectrum. (b) Narrow scan X-ray photoelectron spectra of the I $3d_{5/2}$ region collected following the adsorption of 10 L of iodoethane on a MoAl alloy film at 150 K and heating to various temperatures, where annealing temperatures are marked adjacent to the corresponding spectrum. The spectra were collected after allowing the sample to cool to 150 K. (c) The corresponding XP spectra of C 1s region.

confirms this. This indicates that no stable hydrocarbon species form on this surface at room temperature in contrast to the behavior found on group VIII transition metals [34], where ethylidyne species are stable at this temperature. The low-temperature state clearly corresponds to a weakly bound ethylenic species indicating the presence of some π-bonded ethylene although no infrared modes associated with π-bonded ethylene are detected in RAIRS (Fig. 7(a)). However, the integrated area under the low-temperature state is smaller than that of the high-temperature state so that the coverage of π-bonded ethylene is presumably so low that it cannot be detected in RAIRS.

The data of Figs. 7(b)–(d) indicate that a large proportion of the adsorbed ethylene thermally decomposes to deposit carbon on the surface, which ultimately reacts with the alumina substrate to evolve CO between 1185 and

Table 1
Assignments of the vibrational frequencies for ethyl iodide adsorbed at 80 K on a MoAl surface

Frequency/cm^{-1}	Assignment	Symmetry
3010	CH_2 asymmetric stretch	A
2974	$CH_3 + CH_2$ symmetric stretch	A + A′
2924	CH_3 asymmetric stretch	A′
2965	CH_3 symmetric stretch	A′
1438	CH_3 scissor + CH_3 asymmetric deformation + CH_3 symmetric deformation	A + A′
1373	CH_3 symmetric deformation	A′
1202	CH_2 wag	A′

1220 K. Fig. 2 shows that this dehydrogenation reaction occurs between 300 and 500 K and the hydrogen that is formed reacts with ethylene to yield ethane at ~270 K. Finally, a small amount of methane is detected, indicating the formation of CH_x species during the dissociation of chemisorbed ethylene. Furthermore, adsorption of C_2D_4 results in the formation of CD_4 (at 20 amu) and CHD_3 (at 19 amu) at ~350 K (data not shown) indicating that methyl species are involved in methane formation. However, CH_2D_2 (at 18 amu) is obscured by a background water adsorption so that it is not possible to establish whether methylene species are formed during ethylene dissociation.

Since self-hydrogenation of ethylene is one major reaction pathway on the MoAl alloy (Fig. 2), this reaction was further investigated by studying the chemistry of ethylene on hydrogen-presaturated surfaces. The resulting desorption spectra, displayed in Fig. 3, show desorption of both π- (~170 K) and di-σ-bonded (~280 K) species where there is a slight weakening of the adsorption caused by hydrogen in both cases. Notably, both the ethylene and ethane desorption yields increase substantially in the presence of a saturated overlayer of hydrogen (Fig. 3). The ethane yield evidently increases because of the increased availability of hydrogen, while the increase in the ethylene desorption yield indicates that ethylene decomposition is inhibited by the presence of hydrogen. This effect is emphasized by the data of Fig. 7(d), which show that the amount of carbon remaining on the surface, monitored from the amount of CO that is subsequently evolved, decreases by more than a factor of two on a hydrogen-covered alloy surface. The trailing edge of the 30 amu (ethane) desorption state coincides with the trailing edge of the high-temperature ethylene desorption feature (Fig. 3) indicating that this state is due to hydrogenation of di-σ-bonded ethylene. Evidently, however, some ethane is formed below 200 K (Figs. 2 and 3), indicating that π-bonded ethylene also hydrogenates. In spite of the low yield, since some ethane is detected, it appears that the π-bonded species is extremely active for hydrogenation and must have a very low hydrogenation activation energy. Assuming that the hydrogen coverage is relatively constant at ~260 K, the activation energy for ethylene hydrogenation can be analyzed assuming that it is a first-order reaction to yield a value of ~65 kJ/mol. If π-bonded ethylene hydrogenates with the same activation energy, for the same initial coverage, the yield of the ethane from π-bonded ethylene should be ~1/8000 of that from the di-σ-bonded species. The experimental yields is ~1/7 indicating that the hydrogenation activation energy of the π-bonded species is substantially lower than this value.

The corresponding TPD spectra for a saturated ethylene overlayer (10 L exposure) on a deuterium-saturated surface are displayed in Fig. 4. This shows features at 29–32 amu at ~286 K, corresponding to desorption of ethylene from a hydrogen-covered surface (Fig. 3(b)). Apparently, all ethylene isotopomers up to C_2D_4 are formed with significant intensity. In principle, two different mechanisms can be applied to explain the extensive H–D exchange found here. First, the initial dehydrogenation step of di-σ-bonded ethylene could be reversible so that hydrogen initially lost by dehydrogenation is rapidly replenished by surface hydrogen (deuterium). If this is the case, a vinyl ($C_2H_{3(ads)}$) intermediate may be involved. On the other hand, this chemistry can be achieved through a rapid olefin–alkyl–olefin surface interconversion suggested previously for ethylene on Pt [35] and higher hydrocarbons on Pt [36] and Fe [37]. If this is the case, an ethyl ($C_2H_{5(ads)}$) intermediate is involved. It is found that ethane is also formed at between ~262 and 271 K depending on the ethylene isotopomer that is formed, where all products up to C_2D_6 are detected (Fig. 4). This suggests that an ethyl intermediate is responsible for the H–D exchange reactions, indicated by the very close desorption temperatures of ethylene and ethane isotopomers, and the fact that ethyl species are involved in ethane formation.

In order to explore the hydrogenation pathway in greater detail, the surface chemistry of the ethyl intermediate to ethane formation is investigated by studying iodoethane on the MoAl alloy surface. The infrared spectrum collected following iodoethane adsorption at 80 K is shown in Fig. 8(a). These features can be assigned to molecular iodoethane and the assignments are given in Table 1. Heating to ~150 K causes these feature to sharpen indicating that the overlayer becomes more ordered as it is annealed, and the appearance of an additional feature at ~1425 cm^{-1} suggests the formation of some surface ethyl species [38,39]. Heating to ~200 K and slightly higher causes substantial changes to the infrared spectrum, where all features due to iodoethane and surface ethyl species have disappeared and a features appears at ~1100 cm^{-1}. Comparison with the infrared spectrum of ethylene on the MoAl alloy (Fig. 7(a)) indicates that this is due to di-σ-bonded ethylene. This strongly suggests that, following β-hydride elimination of ethyl species,

a portion of the resulting ethylene does not desorb immediately and stays on the surface until higher temperatures. Note that iodoethane desorption is detected above 200 K from TPD (Fig. 5(a)) while this is not detected in RAIRS (Fig. 8(a)). A similar effect has been found previously on clean and oxygen-modified Mo(1 0 0) [40] and presumably this is because of the drastic difference between sample heating rate where during TPD, the heating rate is ~10 K/s and in RAIRS, the heating rates is substantially lower. The I $3d_{5/2}$ XPS feature shifts from 620.1 eV at ~150 K to ~619.4 eV when the sample is heated to 220 K (Fig. 8(b)), indicating that iodine is lost from the iodoethane to form surface ethyl species and co-adsorbed iodine [39]. C–I bond cleavage for iodomethane [22] and diiodomethane [23] has been found on the same surface at approximately the same temperature. A similar shift in C 1s binding energy (Fig. 8(c)) supports this conclusion. It should be mentioned that recent synchrotron radiation XPS and density functional theory calculations reveal close C 1s binding energies of π- and di-σ-bonded ethylene and a number of other C_2 species including acetylene, vinyl, ethylidene and vinylidene [41]. Our XPS resolution therefore does not allow us to make definite assignments of the adsorbed hydrocarbon species. The intensity of both the I $3d_{5/2}$ and C 1s features attenuate substantially on heating to ~220 K, due to the substantial desorption of iodoethane over this temperature range (Fig. 5(a)). The ethylene species formed on the surface via a β-hydride elimination reaction (Fig. 8(a)) desorbs molecularly at ~280 K (Fig. 5(c)). At the same time, some 30 amu (ethane) signal is detected, presumably due to the hydrogenation of adsorbed ethyl species, while the infrared spectrum shows that no ethyl species are detected on the surface at 200 K (Fig. 8(a)). However, as emphasized by the inset to Fig. 5(c), the amount of molecular iodoethane and ethane desorbing from the surface is substantially lower than the ethylene yield; β-hydride elimination is the predominant reaction pathway for adsorbed ethyl species in the absence of hydrogen.

The effect of a saturated overlayer of hydrogen or deuterium on the chemistry of ethyl species on the MoAl alloy is shown in Fig. 6. Reaction with hydrogen yields a relatively broad 30 amu (ethane) feature centered at ~210–240 K depending on iodoethane exposure, ascribed to the hydrogenation of ethyl species. This temperature is lower than that at which di-σ-bonded ethylene hydrogenates (~260 K, Fig. 3) indicating that, for the hydrogenation of the di-σ-bonded species, the ethyl species reacts more rapidly than the overall ethylene hydrogenation rate implying that, in this case, addition of hydrogen to di-σ-bonded ethylene to form an ethyl species is slower than the rate at which the ethyl species is hydrogenated. However, due to facile β-hydride elimination from ethyl species to form di-σ-bonded ethylene on the surface (Figs. 5(c) and 8(a)), the possibility that some ethylene also hydrogenates to form ethane cannot be ruled out (Fig. 6(a)). This issue is addressed on a D_2-covered surface (Fig. 6(b)) where it is found that, while the 30- and 31-amu profiles show two desorption states, those at 32 and 33 amu have only one. It is rather straightforward to assign the low-temperature desorption state to ethyl hydrogenation where ethyl species originate from C_2H_5I dissociation, while the assignment of the high-temperature desorption state is more difficult. However, it is found that the 32 amu profiles have a desorption maximum at ~310 K, while the 33-amu profiles having a desorption maximum at ~300 K. This situation is very similar to that observed in Fig. 4 so that in this case, we again assign the 32-amu feature to C_2D_4 desorption and that at 33 amu to partially deuteriated ethane. The high-temperature desorption at 30 and 31 amu is therefore assigned to partially deuteriated ethylene. Weak desorption at 34–36 amu is also detected (not plotted) at temperatures slightly lower than 300 K, identical to that found in Fig. 4, indicating all ethane isotopomers up to C_2D_6 are formed. It should be mentioned, however, the desorption temperatures of ethylene and ethane isotopomers starting from $C_2H_5I + D_2$ (Fig. 6(b)) are ~20 K higher than from $C_2H_4 + D_2$ (Fig. 4). There could be two origins for this discrepancy. First, the availability of surface H (D) might be different in the two situations. It is found, following 1 L C_2H_4 or C_2H_5I exposure to a hydrogen-presaturated surface, that the hydrogen yields are very different where it is found that H_2 yield in the latter case is only ~53% of the former. This suggests that the adsorption of C_2H_5I on the surface results in substantial displacement of adsorbed H atoms compared with that of C_2H_4 adsorption (if any). The same conclusion is reached on deuterium-covered surfaces where, in this case, a combination of the yields of both HD and D_2 following C_2H_5I adsorption is also less than that after C_2H_4 adsorption. The decreased availability of surface D atoms may slow down H–D exchange and result in higher desorption temperatures of ethylene and ethane isotopomers. Second, the co-adsorption of iodine atoms on the surface may also result in higher ethylene/ethane desorption temperatures. Iodine adsorption, in principle, may block certain surface sites where di-σ-bonded ethylene dissociates. It has recently been found [22,23] that adsorbed iodine atoms easily oxidize surface aluminum so that the alloy surface is modified electronically and this may also cause higher desorption temperatures of deuteriated ethylene and ethane.

The results shown here and recent studies of iodomethane [22] and diiodomethane [23] all emphasize the different reactivities of the alloy thin film and metallic molybdenum. In terms of ethylene hydrogenation, weak ethane desorption has been found on bare and H_2-covered Mo(1 0 0) at below 200 K [42]. No ethane desorption has been reported on Mo(1 1 0) [43]. The major reaction pathway of ethylene on Mo signal crystal surfaces at above 200 K is complete dissociation to deposit carbon on the surface, together with H_2 evolution. The reaction mechanism, derived from ultraviolet photoelectron [44] and high-resolution electron energy loss [43] spectroscopies, is acetylene formation followed by further dissociation. The decomposition pathway of ethylene on the alloy surface is not clear.

The detection of methane suggests that the decomposition involves CH_x formation. Nevertheless, a much weaker interaction between adsorbed ethylene and the surface is found for the alloy thin film where a portion of adsorbed ethylene, instead of dissociating completely, desorbs at around room temperature. A direct consequence of this is the hydrogenation of di-σ-bonded ethylene, indicated by desorption of ethane at temperatures slightly lower than that of the desorption of ethylene itself. For H–D exchange reactions, it has previously been found that, following CH_3I adsorption on a D_2-covered alloy surface, all methane isotopomers up to CD_4 are formed [22]. This clearly indicates C–H bond dissociation and recombination. In the present study, we observed extensive H–D exchange in ethylene, which is suggested to proceed via a fast ethylene–ethyl–ethylene interconversion process. Again this is drastically different from the chemistry on molybdenum single crystal surfaces where H–D exchange reactions do not occur [45]. Indeed, the hydrogenation and H–D exchange reactions presented here closely resemble the chemistry on Pt single crystal surfaces [46]. This suggests that alloying with aluminum enables molybdenum to gain electrons to such an extent that the catalytic properties are modified to resemble those of late transition metals [22,23].

5. Conclusions

Two forms of ethylene are detected on a MoAl alloy formed on an alumina thin film on a molybdenum substrate consisting of di-σ- and π-bonded ethylene. The di-σ-bonded ethylene has a σ/π parameter of ~0.8 and a heat of adsorption of ~70 kJ/mol. The majority of the adsorbed ethylene dehydrogenates to deposit carbon on the surface, the remainder desorbing molecularly or hydrogenating to yield ethane. A small amount of methane is also detected. Experiments in which ethylene is adsorbed on a hydrogen-saturated surface reveal a hydrogenation activation energy for di-σ-bonded ethylene of ~65 kJ/mol, while π-bonded ethylene hydrogenates substantially more easily.

Adsorbed ethyl species on the MoAl alloy, formed by the thermal decomposition of ethyl iodide, predominantly undergo β-hydride elimination to yield ethylene, or undergo self-hydrogenation to form a small amount of ethane. Adsorbing ethyl species on a hydrogen-saturate surface yields ethane at a lower temperature than that at which di-σ-bonded ethylene hydrogenates indicating that addition of hydrogen to di-σ-bonded ethylene to form ethyl species is slower than the rate of ethyl hydrogenation.

Acknowledgments

We gratefully acknowledge support of this work by the Chemistry Division of the National Science Foundation under grant number CTS-0105329. One of us (YW) would like to acknowledge a dissertator fellowship from the University of Wisconsin-Milwaukee.

References

[1] A. Brenner, J. Mol. Catal. 5 (1979) 157.
[2] E. Davie, D.A. Whan, C. Kemball, J. Catal. 24 (1972) 272.
[3] J. Smith, R.F. Howe, D.A. Whan, J. Catal. 34 (1974) 191.
[4] R. Thomas, J.A. Moulijn, J. Mol. Catal. 15 (1982) 157.
[5] A. Brenner, R.L. Burwell Jr., J. Am. Chem. Soc. 97 (1975) 2565.
[6] A. Brenner, R.L. Burwell Jr., J. Catal. 52 (1978) 353.
[7] R.F. Howe, Inorg. Chem. 15 (1976) 486.
[8] A. Kazusaka, R.F. Howe, J. Mol. Catal. 9 (1980) 183.
[9] K.P. Reddy, T.L. Brown, J. Am. Chem. Soc. 117 (1995) 2845.
[10] A. Zecchina, E.E. Platero, C.O. Areán, Inorg. Chem. 27 (1988) 102.
[11] R.F. Howe, I.R. Leith, J. Chem. Soc. Faraday Trans. I 69 (1973) 1967.
[12] W.M. Shirley, B.R. McGarvey, B. Maiti, A. Brenner, A. Cichowlas, J. Mol. Catal. 29 (1985) 259.
[13] M. Kaltchev, W.T. Tysoe, J. Catal. 193 (2000) 29.
[14] M. Kaltchev, W.T. Tysoe, J. Catal. 196 (2000) 40.
[15] Y. Wang, F. Gao, M. Kaltchev, D. Stacchiola, W.T. Tysoe, Catal. Lett. 91 (2003) 83.
[16] Y. Wang, F. Gao, M. Kaltchev, W.T. Tysoe, J. Mol. Catal. A: Chem. 209 (2004) 135.
[17] Y. Wang, F. Gao, W.T. Tysoe, J. Mol. Catal. A: Chem. 236 (2005) 18.
[18] Y. Wang, F. Gao, W.T. Tysoe, J. Mol. Catal. A: Chem. 235 (2005) 173.
[19] Y. Wang, F. Gao, W.T. Tysoe, J. Mol. Catal. A: Chem., in press.
[20] F. Zaera, Chem. Rev. 95 (1995) 2651.
[21] B.E. Bent, Chem. Rev. 96 (1996) 1361.
[22] Y. Wang, F. Gao, W.T. Tysoe, Surf. Sci. 590 (2005) 181.
[23] Y. Wang, F. Gao, W.T. Tysoe, J. Phys. Chem. B 109 (2005) 15497.
[24] H.S. Guo, F. Zaera, Surf. Sci. 547 (2003) 284.
[25] H.S. Guo, F. Zaera, J. Phys. Chem. B 108 (2004) 16220.
[26] Y. Chauvin, J.-L. Hérisson, Makromol. Chem. 141 (1971) 161.
[27] M. Siaj, P.H. McBreen, Science 309 (2005) 588.
[28] M. Siaj, C. Reed, S.T. Oyama, S.L. Scott, P.H. McBreen, J. Am. Chem. Soc. 126 (2004) 9514.
[29] I. Horiuti, M. Polanyi, Trans. Faraday Soc. 30 (1934) 1164.
[30] W.J. Wytenburg, R.M. Lambert, J. Vac. Sci. Technol. A 10 (1992) 3597.
[31] M. Kaltchev, W.T. Tysoe, Surf. Sci. 430 (1999) 29.
[32] P.A. Redhead, Vacuum 12 (1962) 203.
[33] D. Stacchiola, L. Burkholder, W.T. Tysoe, Surf. Sci. 511 (2002) 215.
[34] R. Deng, E. Herceg, M. Trenary, Surf. Sci. 560 (2004) L195.
[35] T.V.W. Janssens, F. Zaera, Surf. Sci. 344 (1995) 77.
[36] D. Chrysostomou, F. Zaera, J. Phys. Chem. B 105 (2001) 1003.
[37] M.L. Burke, R.J. Madix, J. Am. Chem. Soc. 113 (1991) 4151.
[38] D. Sung, A.J. Gellman, Surf. Sci. 551 (2004) 59.
[39] F. Solymosi, L. Bugyi, A. Oszkó, Langmuir 12 (1996) 4145.
[40] G. Wu, M. Kaltchev, W.T. Tysoe, Surf. Rev. Lett. 6 (1999) 13.
[41] M. Sock, A. Eichler, S. Surnev, J.N. Andersen, B. Klötzer, K. Hayek, M.G. Ramsey, F.P. Netzer, Surf. Sci. 545 (2003) 122.
[42] G. Wu, B. Bartlett, W.T. Tysoe, Surf. Sci. 383 (1997) 57.
[43] B. Fruhberger, J.G. Chen, J. Am. Chem. Soc. 118 (1996) 11599.
[44] L.P. Wang, W.T. Tysoe, Surf. Sci. 236 (1990) 325.
[45] G.F. Wu, H. Molero, W.T. Tysoe, Surf. Sci. 397 (1998) 179.
[46] F. Zaera, J. Phys. Chem. 94 (1990) 8350.